Earth and Planetary Science Letters 364 (2013) 168–179

Contents lists available at SciVerse ScienceDirect

Earth and Planetary Science Letters

journal homepage: www.elsevier.com/locate/epsl

Frontiers Paper

Why do mafic arc magmas contain ~4 wt% water on average?

Terry Plank [a,*], Katherine A. Kelley [b], Mindy M. Zimmer [c], Erik H. Hauri [d], Paul J. Wallace [e]

[a] Lamont-Doherty Earth Observatory of Columbia University, Palisades, NY 10960, USA
[b] Graduate School of Oceanography, University of Rhode Island, Narragansett Bay Campus, Narragansett, RI 20882, USA
[c] Los Alamos National Laboratory, Los Alamos, NM, USA
[d] Department of Terrestrial Magnetism, Carnegie Institution of Washington, Washington DC 20015, USA
[e] Department of Geological Sciences, University of Oregon, Eugene, OR 97403, USA

ARTICLE INFO

Article history:
Received 23 July 2012
Received in revised form
20 November 2012
Accepted 20 November 2012
Editor: T.M. Harrison

Keywords:
melt inclusions
subduction
volatiles
mantle melting
magma chamber
eruption

ABSTRACT

The last 15 yr have seen an explosion of data on the volatile contents of magmas parental to arc volcanoes. This has occurred due to the intense study of melt inclusions trapped in volcanic phenocrysts, aliquots of magma that have presumably escaped degassing during eruption. The surprising first-order result is the narrow range in H_2O concentrations in the least degassed melt inclusions from each volcano. Nearly all arc volcanoes are sourced with mafic magmas that contain 2–6 wt% H_2O. The average for each arc varies even less, from 3.2 (for the Cascades) to 4.5 (for the Marianas), with a global average of 3.9 ± 0.4 wt% H_2O. Significant variations occur from volcano to volcano within each arc, but the means are indistinguishable within one s.d. The narrow range and common average value for H_2O are in stark contrast to the concentrations of most other subduction tracers, such as Nb or Ba, which vary by orders of magnitude. A modulating process, either in the crust or mantle, is likely responsible for the restricted range in the H_2O contents of arc melt inclusions. One possibility is that melt inclusion H_2O values reflect vapor saturation at the last storage depth in the crust prior to eruption. In this scenario, magmas rise from the mantle with variable H_2O contents (>4 wt%), become vapor-saturated and start degassing, and continue to degas up until the depth at which they stall. If the stalling depths are ~6 km, which is common for storage depths beneath volcanoes, magmas would be saturated at ~4 wt% H_2O, and melt inclusions, most of which become closed during further ascent, would thus record ≤ 4 wt% H_2O. Another possibility is that the mantle melting process modulates water content in the melt such that magmas rise out of the mantle with ~4 wt% H_2O. A strong relationship between the water content of the source, $H_2O_{(o)}$ and the degree of melting (F) maintains nearly constant water contents in the melt for a restricted range in mantle temperature. Magmas with 3–4 wt% H_2O can be generated at ~50° below the dry solidus for a wide range in F and $H_2O_{(o)}$. The narrow range in wedge temperatures may be another manifestation of a planet with average upper mantle of 1400 °C potential temperature. The characteristic mean and range of H_2O contents of arc magmas has implications for both the volatile fuel for explosive eruptions and the mass balance of H_2O recycled through subduction zones.

1. Introduction

Water affects every part of a magma's history, from its origins in the mantle to its eruption from a volcano. Water dramatically lowers the solidus temperature of the mantle, and so drives melting (e.g., Katz et al., 2003). It has a major effect on the rheological properties of both magmas and crystals, depolymerizing melt and weakening olivine (e.g., Gonnermann and Manga, 2007; Hirth and Kohlstedt, 1996). Water cycles chemical components between the hydrosphere, mantle, and crust at subduction zones (e.g., Wallace, 2005; Ruscitto et al., 2012). Magmas crystallize and differentiate in unique ways when water is a major dissolved component (e.g., Grove et al., 2003; Zimmer et al., 2010). And water exsolves dramatically from melt at low pressure, causing the vesiculation which fuels explosive eruptions (e.g., Cashman, 2004).

Despite these critical phenomena, the quantitative measurement of the concentration of water in magmas has been an on-going challenge in igneous petrology. The primary difficulty stems from the near complete degassing of magmas during ascent, eruption and cooling. The only bits of magma that escape such near-complete degassing at the surface of the earth are trapped inside crystals. Roberto Clocchiatti, Alfred Anderson and Alexander Sobolev pioneered the petrological utility of such melt

* Corresponding author. Tel.: +1 845 365 8410; fax: +1 845 365 8155.
E-mail addresses: tplank@ldeo.columbia.edu (T. Plank), kelley@gso.uri.edu (K.A. Kelley), mindy.zimmer@gmail.com (M.M. Zimmer), ehauri@ciw.edu (E.H. Hauri), pwallace@uoregon.edu (P.J. Wallace).

0012-821X/$ - see front matter © 2012 Elsevier B.V. All rights reserved.
http://dx.doi.org/10.1016/j.epsl.2012.11.044

inclusions (e.g., Clocchiatti, 1968; Clocchiatti et al., 1975; Anderson 1973, 1976; Sobolev et al., 1983) and this, together with experimental phase equilibrium (see Grove et al. (2012)), are the primary approaches used today for determining pre-eruptive volatile contents of magmas. Another hurdle is in the quantitative measurement of H_2O or H species in such inclusions. Early inferences were based on the absence of measurement—the deficit from 100% on the sum of the oxides measured by electron microprobe. Such sum deficits were not very precise, but they turned out to provide an accurate view of the water-rich nature of arc magmas. FTIR and SIMS ion microprobe techniques now provide higher precision and information on H speciation.

In the mid-90s, a series of seminal papers brought these new analytical methods to melt inclusion and submarine glass studies of subduction zone magmas (Danyushevsky et al., 1993; Sisson and Layne, 1993; Stolper and Newman, 1994; Sobolev and Chaussidon, 1996; Roggensack et al., 1997). Together, this work demonstrated unequivocally that subduction zone magmas are initially wet, with primary water concentrations being at least 2 wt%, and more evolved basalts containing up to 6 wt% H_2O. The new techniques developed in these papers spawned a flurry of studies on magmatic water, leading to a wave of new understanding on subduction water fluxes (Sadofsky et al., 2008; Ruscitto et al., 2012), wet melting in the mantle (Kelley et al., 2006, 2010; Langmuir et al., 2006; Portnyagin et al., 2007; Johnson et al., 2009; Ruscitto et al., 2010), cross-arc water variations (Walker et al., 2003) the ascent of arc magmas (Blundy and Cashman, 2005), their differentiation (Zimmer et al., 2010) and eruption (Blundy et al., 2006; Metrich et al., 2010; Spilliaert et al., 2006). Complementary phase equilibria studies also supported very high water contents in some parental arc magmas (6–16 wt% H_2O; Grove et al., 2005; Carmichael, 2002). The future will see further development of Raman spectroscopy, with single micron spatial resolution on unexposed inclusions (Mercier et al., 2010), and nanoSIMS, with the potential for single micron spatial resolution and single ppm detection limits in nominally anhydrous phenocrysts (Hauri et al., 2011; Mosenfelder et al., 2011).

Approximately 15 yr later, focused efforts by many groups have now provided baseline data for a number of volcanic arcs. The surprising result is how little the H_2O concentration varies in the least degassed mafic melts from each volcano. The purpose of this paper is to present this observation, and then explore mechanisms that could lead to similar average water contents for different arcs.

2. The data

Magmas lose their dissolved H_2O as a natural consequence of ascent and eruption. A magma with 7 wt% H_2O (the maximum observed in olivine-hosted inclusions, from Klyuchevskoy, Kamchatka; Auer et al., 2009 and Augustine, Alaska; Zimmer et al., 2010) will reach pure H_2O-vapor saturation at ~400 MPa, or ~15–16 km in the crust (assuming an upper crustal density of 2.6 g/cc, and using the solution models of Newman and Lowenstern (2002) and Witham et al. (2012)). As magmas ascend to depths shallower than their point of H_2O-saturation, they will continually degas H_2O to vapor, striving to reach equilibrium during decompression, eruption, and cooling. At the earth's surface (1 atm pressure), mafic melts can hold ~0.1 wt% H_2O. Thus, all wet magmas lose H_2O to vapor upon ascent; only melt inclusions trapped in early formed crystals that are brought to the surface and cooled rapidly stand some chance of preserving original H_2O concentrations. Olivine is the vessel of choice, as it is one of the first minerals to crystallize in arc basaltic magma, and contains minor concentrations of incompatible elements that can exchange with melt inclusions. Clinopyroxene-hosted melt inclusions or phenocrysts themselves may also preserve information about undegassed water concentrations (Zimmer et al., 2010; Wade et al., 2008). Tephra clasts ≥3 cm in diameter cool slowly enough (~10 min) that a significant fraction of H_2O (~1 wt%) may be lost by diffusion through the olivine (Lloyd et al., 2013), and so only melt inclusions in small diameter scoria lapilli or ash retain pre-eruptive H_2O contents. CO_2 and S generally have a lower solubility in arc magmas than H_2O (Wallace, 2005;

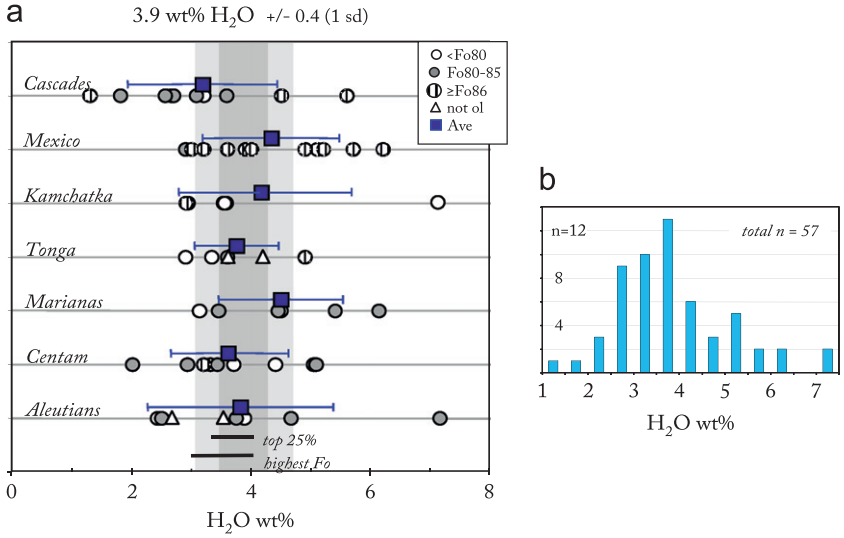

Fig. 1. (a) Water concentration in melt inclusions from 7 volcanic arcs (data and references in Table 1 and Appendix). Each point plotted is the maximum water concentration measured in mafic melt inclusions from a single volcano or cinder cone. Most inclusions are hosted in olivine; symbols reflect forsterite (Fo) content and non-olivine hosts (clinopyroxene and plagioclase). Blue boxes are averages of volcanoes within each arc (error bars are one standard deviation). Grey vertical bar reflects average of all arcs (dark grey is one s.d.; light grey is two). Heavy black lines are global averages (± 1 s.d.) calculated using two other approaches: averaging the top 25% of the water contents within a given melt inclusion population, and selecting the maximum H_2O content within the highest Fo olivines (top 2 Fo units) in a given population. (b) Histogram of maximum water concentrations in each volcano or cinder cone. (For interpretation of the references to color in this figure legend, the reader is referred to the web version of this article.)

Table 1
Maximum H_2O concentrations measured in melt inclusions from arc volcanoes.

Arc	Volcano	H_2O-max[a]	Fo	H_2O-25%[b]	*n*	H_2O-Fo[c]	Fo range	H_2O-90[d]	*n*-Total[e]	Nb[f]	Ba	Sample	References
Aleutians	Augustine	7.15	80.4	6.71	9	6.32	86–84	6.16	38	0.883	134	NY-17	Zimmer et al. (2010); Zimmer (2008)
Aleutians	Emmons	2.50	81	2.31	10	2.02	85–83	2.08	42	3.81	365	G-1	Zimmer et al. (2010); Zimmer (2008)
Aleutians	Shishaldin	2.43	69.1	2.24	5	2.38	72–70	Fo70	22	6.17	310	SPS-31B	Zimmer et al. (2010); Zimmer (2008)
Aleutians	Akutan	3.88	74.7	3.88	1	3.88	74.6–72.6	Fo75	6	1.18	224	RKAK1	Zimmer et al. (2010); Zimmer (2008)
Aleutians	Unalaska	3.54	84.7 cpx	2.89	6	3.21	88.7–86.7	3.07	26	1.17	195	ave MI	Zimmer et al. (2010); Zimmer (2008)
Aleutians	Okmok	2.68	80.6 cpx	2.50	3	2.46	85–83 cpx	2.21	14	2.97	255	01NY-010	Zimmer et al. (2010); Zimmer (2008)
Aleutians	Korovin	4.66	80	4.30	3	4.59	82.3–80.3	3.85	14	3.24	422	404T5	Zimmer et al. (2010); Zimmer (2008)
Aleutians	Seguam	3.75	83.5	3.37	5	3.75	85.4–83.4	3.32	22	1.02	173	SEG07-05	Zimmer et al. (2010); Zimmer (2008)
Aleutians	**Average**	**3.82**		**3.53**		**3.58**		**3.45**		**2.55**	**260**		
	StDev	*1.6*		*1.5*		*1.4*		*1.5*		*1.9*	*99*		
Centam	Fuego	4.35	76.3	4.14	5	4.35	76.2–74.2	Fo73	22	1.62	320	VF74-169	Lloyd et al. (2013); Plank (2005)
Centam	Cerro Negro	5.08	81.1	5.07	2	5.07	82.6–80.6	4.25	10	1.32	391	CN-92-2	Sadofsky et al. (2008)
Centam	Arenal	3.70	76	3.65	4	3.56	79–77	Fo76	18	2.77	325	AR0302	Wade et al. (2006)
Centam	Irazu	3.20	87	3.18	1	3.18	85–87	3.05	6	23.0	857	IZ03-17a	Benjamin et al. (2007)
Centam	Santa Maria	3.31	79	3.31	1	3.31	79.5–77.5	Fo79	6	3.50	410	GU-19d-s1	Sadofsky et al. (2008)
Centam	Atitlan	3.20	75.4	3.20	1	3.20	75.4–73.4	Fo75	6	3.80	460	GU-25b-s1	Sadofsky et al. (2008)
Centam	Agua	3.43	81.1	3.43	1	3.43	81.1–79.1	2.99	6	2.40	369	GU-11d-s1	Sadofsky et al. (2008)
Centam	Telica	2.93	80.2	2.93	1	2.93	80	2.42	6	1.20	680	P2-16-9	Sadofsky et al. (2008)
Centam	Nejapa	2.01	83	2.02	1	2.02	83.1–81.1	1.71	6	3.20	89	ave MI	Sadofsky et al. (2008)
Centam	Granada	5.04	78.8	5.04	1	3.59	87.3–85.3	3.67	6	2.00	302	P2-58-2-7	Sadofsky et al. (2008)
Centam	**Average**	**3.63**		**3.60**		**3.46**		**3.02**		**4.48**	**420**		
	StDev	*0.96*		*0.94*		*0.81*		*0.90*		*6.6*	*212*		
Marianas	Agrigan	5.40	80	5.29	2	5.40	81.6–79.6	4.38	10	1.19	220	AGR19	Shaw et al. (2008); Kelley et al. (2010)
Marianas	Pagan	3.45	80	2.95	2	3.45	80.5–78.5	2.99	10	0.95	214	PB64	Shaw et al. (2008); Kelley et al. (2010)
Marianas	Sarigan	6.13	82.5	5.56	2	4.99	86.1–84.1	5.20	10	1.64	235	SA-93, Sari-15–02	Shaw et al. (2008); Kelley et al. (2010)
Marianas	Guguan	4.49	75	3.85	4	3.11	81.2–79.2	3.32	18	0.52	106	GUG-79-1	Shaw et al. (2008); Kelley et al. (2010)
Marianas	Asuncion	4.45	82	4.34	2	4.45	81.9–79.9	3.77	10	0.95	193	Asun-20-01	Shaw et al. (2008)
Marianas	Alamagan	4.45	83.7	4.45	1	4.45	85.6–83.6	3.97	6	1.06	195	ALA-01	Shaw et al. (2008)
Marianas	Anatahan	3.13	68.3	3.13	1	3.13	68.5–66.5	Fo68	6	1.20	210	Anat-4	Shaw et al. (2008)
Marianas	**Average**	**4.50**		**4.22**		**4.14**		**3.94**		**1.07**	**196**		
	StDev	*1.04*		*1.00*		*0.92*		*0.79*		*0.34*	*42*		
Tonga	Volcano L (N)	3.60	85	3.24	4	3.11	90.1–88.1	3.32	18	0.876	117	VLND7101	Cooper (2009)
Tonga	Volcano D	2.90	72	2.90	1	0.93	77.4–75.4	Fo72	6	0.198	91	VDND2301	Cooper (2009)
Tonga	Tofua	4.20	90.3 cpx	3.51	3	4.16	90.3–88.3	3.61	14	0.211	128	06TF70	Cooper (2009); Caulfield et al. (2012)
Tonga	Volcano A	4.90	88.9	4.62	4	3.92	92.2–90.2	4.17	18	0.100	101	VAND0401	Cooper et al. (2010)
Tonga	Volcano 7	3.62	An 95	3.25	2	3.30	76.3–74.3	2.86	10	0.450	120	V7TD5801	Cooper (2009)
Tonga	Volcano 19 (S)	3.34	70	3.27	2	1.60	81.0–79.0	Fo70	10	0.427	94	V19T0301	Cooper (2009)
Tonga	**Average**	**3.76**		**3.47**		**2.84**		**3.49**		**0.377**	**108**		
	StDev	*0.70*		*0.60*		*1.3*		*0.55*		*0.28*	*15*		
Kamchatka	Ksudach	3.55	76.6	3.55	1	3.16	81–79	2.58	6	0.902	62	Inc 47-1	Portnyagin et al. (2008)
Kamchatka	Chikurachki	3.53	74.2	3.45	3	3.53	75.1–73.1	Fo74	14	1.34	194	CHK13-1, 1-2	Portnyagin et al. (2008)
Kamchatka	Karymsky	3.58	72	3.58	1	3.25	81.8–79.8	2.75	6	2.89	316	5MPKB106	Portnyagin et al. (2008)
Kamchatka	Tolbachik	2.91	88	2.88	2	2.81	90.8–88.8	2.81	10	1.70	270	TOL-30-9	Portnyagin et al. (2008)
Kamchatka	Kliuchevskoy	7.10	80	5.16	5	1.64	88.3–86.3	2.69	22	1.30	241	s300/63	Auer et al. (2009)
Kamchatka	**Average**	**4.13**		**3.72**		**2.88**		**2.71**		**1.63**	**217**		
	StDev	*1.7*		*0.85*		*0.74*		*0.10*		*0.76*	*97*		
Mexico	Paricutin	4.90	86.1	4.80	2	4.90	87.4–85.4	4.50	10	4.90	254	incl P506-10	Johnson et al. (2009)
Mexico	Popo	5.10	88.3	5.00	2	5.10	89.8–87.8	4.95	10	7.24	241	M28-2 gr5 incl	Roberge et al. (2009)
Mexico	Jorullo	5.70	90.1	4.50	4	5.40	91.1–89.1	5.70	18	3.00	222	WR-early	Johnson et al. (2008)
Mexico	Jumiltepec	3.00	88.2	3.00	1	3.00	88.2	2.97	6	4.00	444	MI	Cervantes and Wallace (2003)
Mexico	Las Tetillas	3.60	87.8	3.60	1	3.60	87.8	3.53	6	3.00	169	MI	Cervantes and Wallace (2003)
Mexico	Tuxtepec	5.20	89.6	5.20	1	5.20	89.6	5.20	6	4.00	1453	MI	Cervantes and Wallace (2003)

Mexico	Tepetlapa	3.20	87.5	3.20	1	3.20	87.5	3.13	6	16.00	305	MI	Cervantes and Wallace (2003)
Mexico	Colima	6.20	89.3	4.28	5	6.20	90.9–88.9	6.08	22	7.70	1548	AP-01-Bas-WR	Vigouroux et al. (2008)
Mexico	San Juan	2.90	84.6	2.88	4	2.90	83–85	2.40	18	10.90	291	Bulk tephra	Johnson et al. (2009)
Mexico	Hungaro	3.90	87	3.90	1	3.90	88.2–86.2	3.80	6	3.95	255	Bulk tephra	Johnson et al. (2009)
Mexico	Asterillo	4.00	88.6	4.00	1	4.00	89.4–87.4	3.80	6	3.30	198	Bulk tephra	Johnson et al. (2009)
Mexico	**average**	**4.34**		**4.03**		**4.31**		**4.19**		**6.18**	**489**		
	StDev	*1.1*		*0.80*		*1.1*		*1.2*		*4.1*	*506*		
Cascades	Whaleback (SH)	5.60	94	4.02	1	5.60	94–92	5.60	6				Ruscitto et al. (2011); Anderson (1974a,b, 1979)
Cascades	Goosenest (SH)	3.20	78.4		1	2.60	81–79	Fo78	6				Sisson and Layne (1993)
Cascades	Copco (SH)	1.30	85.9		1	1.30	85.5–86.3	1.16	6				Sisson and Layne (1993)
Cascades	Sargent (SH)	4.50	88	4.50	1	4.50	88	4.33	6				Anderson (1974b)
Cascades	TwinCraters	1.81	83.7	1.76	2	1.81	84–82	1.57	10	5.20	415	TC063Abottom	Ruscitto et al. (2010)
Cascades	SandMnt	2.56	84.02	2.37	2	2.56	84.8–82.8	2.25	10	10.10	381	SM2	Ruscitto et al. (2010)
Cascades	Island Fissure	2.66	82.2	2.44	3	2.66	83.2–81.2	2.25	14	13.28	424	1-PT05-h1	Ruscitto et al. (2010)
Cascades	Yapoah	3.08	82.3	3.05	2	3.08	84.0–82.0	2.66	10	3.30	242	Yo061E	Ruscitto et al. (2010)
Cascades	Collier	2.70	83.2	2.70	1	2.70	84.6–82.6	2.39	6	4.00	301	EJYo2 (Surface)	Ruscitto et al. (2010)
Cascades	BlueLake	3.59	82	3.53	3	3.54	84.2–82.2	3.07	14	3.70	229	Bomb W.R.	Ruscitto et al. (2010)
	Average	**3.19**		**3.45**		**3.11**		**3.03**		**6.60**	**332**		
	StDev	*1.2*		*0.9*		*1.3*		*1.4*		*4.1*	*87*		
Global averages		**3.91**		**3.72**		**3.47**		**3.40**					
		0.45		0.30		0.58		0.53					

[a] H_2O-max is the highest H_2O concentration (wt%) in each volcano; corresponding forsterite (Fo) of olivine host (or Mg# of host cpx or An of host plag) also given.
[b] H_2O-25% is the average H_2O (with *n* analyses in the average) for the top quartile of H_2O concentrations, in melt inclusions screened first for $>$ 500 ppm S.
[c] H_2O-Fo is the average H_2O for melt inclusions hosted in the top 2 Fo units for the population from each volcano; actual range given.
[d] H_2O-90 is the H_2O concentration in melt in equilibrium with Fo_{90} (mantle); calculated from H_2O max and adding equilibrium olivine incrementally until Fo_{90}. Inclusions in Fo $<$ 80 excluded.
[e] *n*-total is total number of melt inclusions from each volcano.
[f] Nb and Ba (ppm) concentration, generally as measured in whole rock (WR) hosts (sample names given), but in some cases (as noted) as measured in melt inclusions (MI).

Benjamin et al., 2007), and so melt inclusions with finite CO_2 (10's to 1000 ppm) and high S (1000's ppm) are minimally degassed and generally preserve the highest H_2O contents. Even so, melt inclusion populations at best record the degassing process, and the maximum H_2O concentration measured is generally taken as a minimum for the primary H_2O content for the magma.

Taking into account these considerations, various approaches have been adopted to infer primary H_2O contents of magmas. Some studies screen melt inclusions based on CO_2 or S thresholds (Kelley et al., 2010), while others backtrack to asymptotic portions of the degassing trends (Benjamin et al., 2007). The simplest approach, however, is to select the maximum H_2O concentration or H_2O/K_2O ratio recorded within a melt inclusion population as representative of the parental magma (Johnson et al., 2009, 2010; Cooper et al., 2012; Ruscitto et al., 2010, 2012), because virtually all processes result in H_2O-loss. This is the approach we have adopted here, employing a few different methods to obtain the highest H_2O contents recorded within a melt inclusion population. The details of these methods are given in Fig. 1, Table 1, and Electronic Supplement. In the compilation, we excluded melt inclusions from lava or bomb samples, as these have generally cooled too slowly to prevent diffusive loss of H_2O, and we excluded volcanoes beyond the main arc volcanic front. The full melt inclusion database represents almost 60 volcanoes, 600–700 individual basaltic or basaltic andesite inclusions, hosted predominantly in olivine.

3. Results

The surprising result is the narrow range and similar averages for the water content of mafic melts from each arc (Fig. 1a). All arc volcanoes have 2–6 wt% H_2O, with few exceptions. There is no simple relationship between H_2O in the melt inclusion, Fo content of the olivine host, nor SiO_2 content of the inferred parental magma (i.e., $Si_{(Fo90)}$; although some relationships may exist within given arcs, Ruscitto et al., 2010; Ruscitto et al., 2012). Nonetheless, arcs which otherwise share no commonality in their tectonic setting or geochemistry (e.g., Tonga and Central America) possess a similar range and average in their inferred H_2O contents. Virtually every arc volcano has a higher H_2O content than any mid-ocean ridge basalt, back-arc basin basalt or ocean island basalt (which have generally $\leq$ 2 wt% H_2O; Zimmer et al., 2010). But the range is surprisingly narrow (2–6 wt% H_2O).

A simple average of the water contents within each arc reveals an even narrower range, from 3.2 (Cascades) to 4.5 (Marianas), and averaging 3.9 $\pm$ 0.4 wt% H_2O (1 s.d.) worldwide. This average is based on the maximum H_2O concentration found from each volcano, then averaged within each arc. A similar result is found using the upper quartile of water contents and only the highest Fo hosts in a given population (Fig. 1a and Table 1). The similarity in these different averaging approaches provides support for the maximum H_2O values being representative of the population, and not being strongly affected by either crystal fractionation or degassing. The average of $\sim$4 wt% is not an artifact resulting from averaging of end-members between 2 and 6 wt%, but reflects a strong peak at 3–4 wt% in the histogram of individual values for each volcano (Fig. 1b).

This common range (2–6 wt%) and average ($\sim$4 wt%) in H_2O contents for mafic arc melts is in stark contrast to most other minor or trace element variations. Fig. 2 plots the Nb and Ba concentrations in the same volcano and arc population as assessed for H_2O. In the case of Ba, which is commonly thought to largely derive from subducted sediments and basaltic oceanic crust, several arcs show non-overlapping means (Tonga, Marianas, Cascades) that vary by more than a factor of four (i.e., from

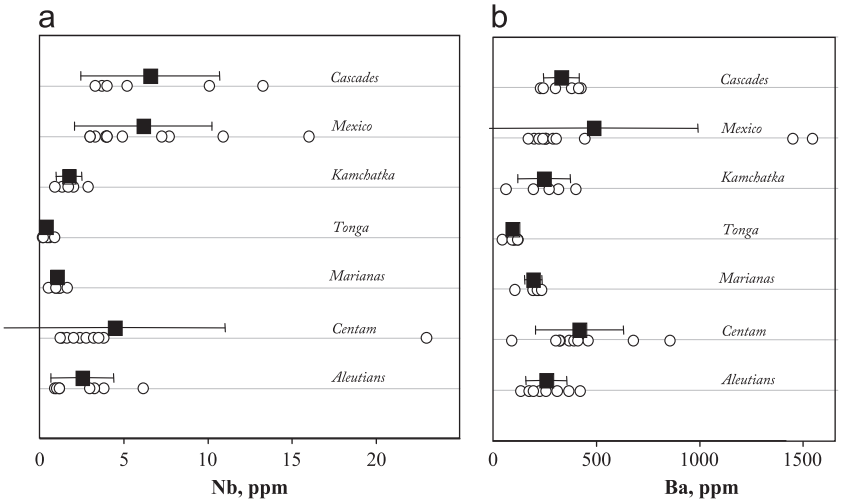

Fig. 2. Nb and Ba concentration in the same samples, volcanoes and arcs as in Fig. 1. Open circles are for each volcano and black boxes are arc averages (± 1 s.d.). Concentrations are in most cases as measured in whole rock tephra; some are as measured directly in melt inclusions. Data sources are given in Appendix.

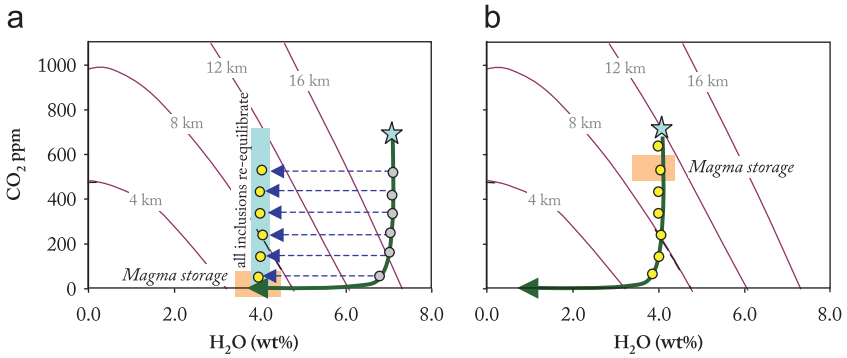

Fig. 3. Two scenarios that produce similar hypothetical melt inclusion arrays (yellow circles) for different initial H_2O and CO_2 concentrations (blue stars). (a) Very water-rich magma rises from >15 km, following a closed-system degassing path (green curve), initially exolving CO_2-rich vapor, then H_2O-rich vapor. The transition to major H_2O loss occurs when the magma reaches the depth of $\sim$pure H_2O saturation ($\sim$12 km). If magma then stalls at 6 km (orange box) for a period of time greater than a few days, melt inclusions that might have formed earlier (grey circles) will re-equilibrate to the vapor-saturated H_2O content of the ambient magma ($\sim$4 wt%), due to the rapid diffusivity of H^+ (but not CO_2) through olivine. Hence, magma storage regions that occur shallower than the point of H_2O saturation will tend to reset melt inclusions to the H_2O content of the host magma, and information about the primary water contents will be lost. (b) The same melt inclusion array could be generated from a magma that had 4% H_2O initially, stalled in a deep magma chamber (10 km), and then ascended rapidly (<1 day) to the surface during eruption. Stalling under H_2O-undersaturated conditions does not lead to a change in H_2O, since there is no difference between the H_2O concentration inside and outside the inclusion. In this case, melt inclusions might faithfully record primary H_2O contents. This will be true for any magma storage regions that form at depths greater than 6 km, including those that form very near 6 km. In fact, there may be a natural tendency for magma to stall at the point of H_2O-saturation, due to the increase in viscosity that occur as H_2O exsolves from the melt and also drives crystallization. These scenarios can be tested by comparing melt inclusion H_2O–CO_2 data to the depths of magma storage constrained from geodetic and seismic observations. Vapor-saturated isobars are from the SolEx model in Witham et al. (2012), and converted to depth assuming 2.6 g/cc upper crustal density. (For interpretation of the references to color in this figure legend, the reader is referred to the web version of this article.)

108 ± 15 ppm Ba for Tonga to 420 ± 212 ppm Ba for Central America), and individual volcanoes vary by more than an order of magnitude (from 62 ppm for Ksudach, Kamchatka to >1500 ppm for shoshonites from Colima, Mexico). Even larger variations are observed for Nb, typically considered a conservative element in subduction zones (i.e., minimal inputs from the subducting slab). Even Ce, which has a similar mantle–melt partition coefficient to H_2O, varies an order of magnitude more than H_2O (Cooper et al., 2012). The large variations in these slab and mantle tracers are not found in H_2O, which instead varies by only a factor of three for 90% of the volcanoes (2–6 wt% H_2O), and $<20\%$ for the average arc values (3.9 ± 0.4 wt% H_2O).

So what processes are responsible for the restricted water variation observed in mafic arc magmas? It seems unlikely that the H_2O input from the subduction zone is the same everywhere, given the strong variations in other tracers, which point to a great variety in composition (e.g., Th/La, Plank, 2005) and flux (e.g., Ba flux; Plank and Langmuir, 1993) that recycle from the subducted slab at different convergent margins. The order of magnitude variation in H_2O/Ce also points to very different fluid compositions, likely equilibrated at different slab surface temperatures, supplying different arcs (Plank et al., 2009; Cooper et al., 2012; Ruscitto et al., 2012). Instead, we look here at two processes that may drive water concentrations in magmas to a narrow range of values: (1) the depth of stalling in the crust, and (2) the extent of melting in the mantle. There is merit to both hypotheses, and future work may provide better tests of them.

4. Crustal control on magmatic water

One possible control on the water content of arc melt inclusions is equilibration within crustal storage regions. For example, magmas could rise from the mantle with variable water contents (>4 wt%), start degassing at the depth of vapor-saturation, and continue to degas up until the depth at which they stall (Figs. 3 and 4). If the stalling depth is shallower than the depth of H_2O-saturation (Fig. 3a), then melt inclusions formed at greater

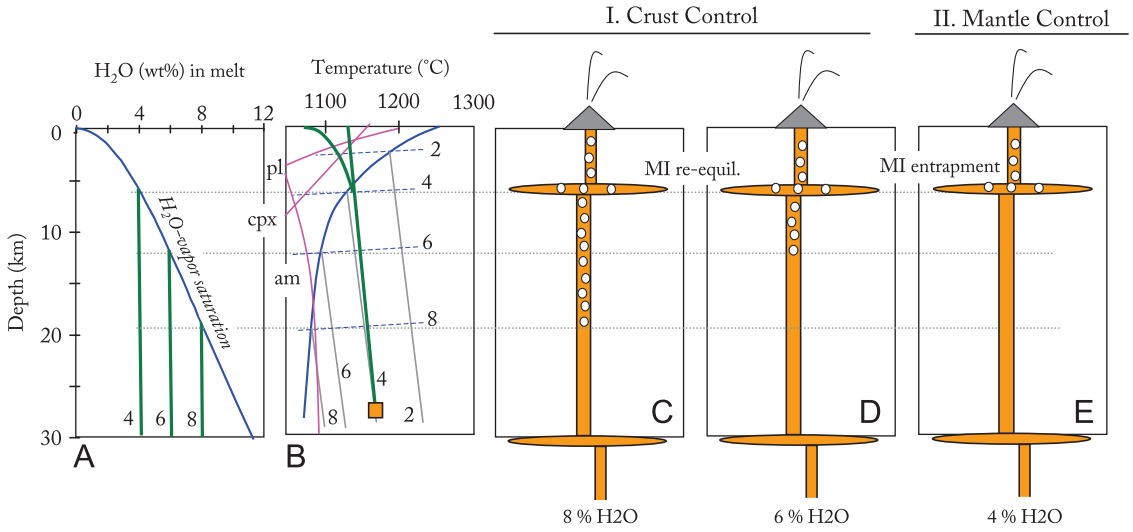

Fig. 4. Crust vs. mantle control on the water concentration in magmas, as recorded in melt inclusions. Panel A gives water solubility in basalt (1100 °C) as a function of pressure (converted to depth assuming 2.6 g/cc upper crustal density), calculated from SolEx (Witham et al, 2012). Panel B is a phase diagram for wet basalt, based on experiments and pMELTS, as in Johnson et al. (2009), Weaver et al. (2011), and Grove et al. (2003). The blue curve is water-saturated and the grey lines are under-saturated liquidi (wt% H_2O labeled). Dashed lines are labeled with water solubility in melt at vapor saturation. Green paths are possible adiabats. Pink lines are plagioclase, clinopyroxene, and amphibole-in crystallization. Initial melt with 4 wt% H_2O begins at orange box, ascends along green adiabat, exsolves bubbles at vapor-saturation (intersecting 4% dashed line), and continues to vesiculate and crystallize to the surface (as for E). Panels C–E illustrate different scenarios by which melt inclusions may record a maximum of 4 wt% H_2O. Magmas ascend from the mantle with dissolved water (vertical lines in panel A) that exsolves at the depth of vapor saturation (bubbles in panels C–E). In the crust control scenario, magmas may originate in the mantle with H_2O >4 wt%, and start to vesiculate at various depths depending on the initial H_2O content (i.e., C vs. D). Crustal structure (a change in the density, rheology or stress state of the crust) then leads to magma stalling at $\sim$6 km, where magma and melt inclusions equilibrate to 4 wt% H_2O (vapor saturation at this point). Rapid ascent and eruption above this depth leads to melt inclusions that record a maximum of 4 wt% H_2O. In the mantle control scenario, magmas originate in the mantle with $\sim$4 wt% H_2O, and stall at 6 km because they reach vapor saturation there. The increase in viscosity of the magma due to water exsolution from the melt, and accompanying crystallization, leads to stalling at this depth. Crystallization here and during further ascent leads to melt inclusion entrapment with 4 wt% H_2O maximum. Illustrations are schematic; real magma plumbing systems are likely highly complex. The presence of other volatiles (e.g., CO_2 and S) will increase vapor saturation pressures; these examples only consider H_2O for simplicity. Ponding at the Moho or in the lower crust may lead to cooling and crystallization of olivine, omitted here for clarity. (For interpretation of the references to color in this figure legend, the reader is referred to the web version of this article.)

depths could re-equilibrate H_2O with the ambient magma in the matter of days, given the rapid equilibration times between melt inclusions and exterior melt through olivine indicated by laboratory and natural experiments (Massare et al., 2002; Portnyagin et al., 2008; Chen et al., 2011; Lloyd et al., 2013; Gaetani et al., 2012). A stalling depth of $\sim$6 km would cause inclusions to reset to $\sim$4 wt% H_2O (i.e., H_2O-saturation at 6 km, or 150–160 MPa; Witham et al., 2012; Newman and Lowenstern, 2002; Fig. 3(a)). Inclusions might still contain variable CO_2, which due to its lower presumed diffusivity in olivine, is unlikely to re-equilibrate. Melt inclusions that formed during subsequent ascent in the volcanic conduit prior to eruption would only record degassing at <6 km depth, trapping melts with lower H_2O contents and little or no CO_2, whereas inclusions that ascended most rapidly from the storage region would preserve the 4 wt% maximum. Such a scenario, a variation on the crustal filter concept, would impose a common H_2O content to melt inclusions (Fig. 4c and d).

The requirement of this process, however, is that an external driver causes H_2O-saturated magmas to stall at $\sim$6 km on average. Such a control could arise from several transitions in the upper crust, such as a ductile to brittle transition. Magmas could also stall due to a change in stress state, favoring sill over dike propagation, or the density structure of the crust could vary such that magmas lose buoyancy. These are all reasonable expectations, and yet it is not entirely clear how these transitions would be so similar in depth for such different volcanic arcs, given different crustal thicknesses (e.g., <20 km for Tonga vs. $\sim$45 km for parts of Mexico; Contreras-Reyes et al., 2011; Johnson et al., 2009), stress states (arcs in extension like Nicaragua vs. compression like segments of the Aleutians) and brittle–ductile transitions (possibly quite different beneath low magma flux cinder cones vs. large edifices with a long history). Some variation is permissible, given the range of water contents typical of most arc magmas: 2–6 wt% H_2O corresponds to 1.5–12 km depth, or 40–300 MPa vapor saturation pressure (for pure H_2O; CO_2 will increase these pressures). Certainly most magma storage regions beneath active arc volcanoes occur in this $\sim$2–12 km range, based on geodetic and seismic observations (e.g., Lu et al., 2010; Cervelli et al., 2010; Scandone et al., 2007). There is also strong evidence that the maximum H_2O content of melt inclusions correlates with geophysically-determined storage depth (Zimmer et al., 2007). With this perspective, an average stalling depth of 6 km (resulting in $\sim$4 wt% H_2O) is consistent with observed magma storage depths.

On the other hand, magmas may stall in the upper crust for reasons intrinsic to the magma, indeed as a consequence of their initial water contents and hence magma viscosity. Wetter magmas that rise from the mantle reach water saturation at greater depths (Fig. 4a), where the exsolution of water would increase viscosity in the melt (which increases with decreasing dissolved water content), and also raise liquidus temperatures and so drive crystallization (Fig. 4b), further increasing magma viscosity. Such an increase in magma viscosity could lead to a decrease in ascent velocity (for a given over-pressure) in a scenario that is similar to, but less lethal than, the viscous death envisioned for silicic plutons by Annen et al. (2006). Magmas with less initial water may rise to shallower depths before reaching H_2O-saturation and viscous stalling. Thus, there could be an intrinsic control on magma storage depth, driven by inherent variations in magma H_2O contents that arise from the mantle, independent of crustal structure and stress state. The implication of this scenario is that the narrow range of water contents observed reflects a narrow range generated in the mantle (Fig. 4e).

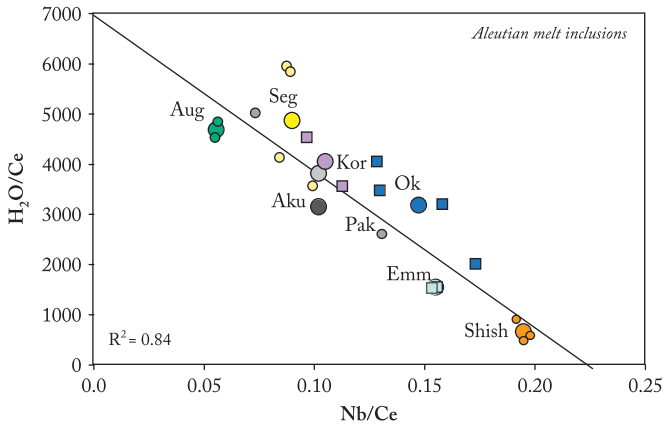

Fig. 5. H_2O/Ce vs. Nb/Ce in melt inclusions from Aleutian volcanoes (Augustine, Seguam, Akutan, Korovin, Okmok, Pakushin, Emmon, and Shishaldin). Large circles are averages of individual melt inclusions (small symbols). Only the inclusions with the highest H_2O contents (least degassed) from each volcano are plotted (H_2O from Zimmer et al. (2010)). Nb and Ce are laser ablation ICPMS analyses of individual melt inclusions (Zimmer, 2008). The strong linear trend is consistent with addition of high H_2O/Ce slab fluid/melt addition to the Aleutian mantle wedge (after Cooper et al. (2012)).

4.1. Testing the crustal control

So do water contents of magmas control the depth of magma storage, or do magma storage depths control water contents? How do we test if the water contents we measure are intrinsic to the primary magma or imposed by stalling depths? One test might involve the degassing paths followed by magmas. Coupled H_2O–CO_2 systematics are useful in constraining the depth of melt inclusion entrapment, and when combined with geodetic or seismic constraints on magma storage depths, have potential to discriminate different degassing and resetting scenarios that may occur in the crust (as outlined in Figs. 3 and 4). Some examples from the Aleutians are given in Electronic Supplement.

Another test involves consideration of the most primitive olivine hosts. Loss of H_2O from melt has a large effect on the olivine liquidus, and inevitably drives crystallization. If magmas originate in the mantle in equilibrium with $\sim Fo_{90}$ olivine, and degas and crystallize in the crust until they stall, then a decrease in H_2O should be accompanied by a decrease in Fo. Thus melt inclusions trapped in the highest Fo olivines should be minimally affected by the crustal filter. Indeed, melt inclusions in $>Fo_{88}$ olivines average a bit higher H_2O (4.6 wt%, $n=11$) than the global value (3.9 wt%), but not substantially (Fig. 1 and Table 1). A similar mean and range (3–6 wt% H_2O) to the global population exists for melt inclusions in these most primitive olivines, and so water concentrations may be set prior to the crustal filter.

Finally, the greatest insights might come from relationships between H_2O and source characteristics of the magma. For example, ratios of incompatible elements in arc magmas generally reflect sources in the subduction zone, the ultimate source of H_2O as well. Degassing in the crust drives H_2O loss, with little effect on trace element ratios, and so would decouple any primary relationships. Such a process may explain why good correlations between H_2O and other slab tracers have been elusive for some arcs, such as the Marianas (Hauri et al., 2007). On the other hand, H_2O contents do appear to correlate with subduction tracers (i.e., Ba/La, Pb/Ce) in Kamchatka, Central America, Mexico and the Cascades (Portnyagin et al., 2007; Sadofsky et al., 2008; Cervantes and Wallace, 2003; Johnson et al., 2009; Ruscitto et al., 2010). Fig. 5 shows a strong relationship between H_2O/Ce and Nb/Ce in Aleutian melt inclusions, consistent with mixing between low H_2O/Ce–high Nb/Ce mantle and a high H_2O/Ce–low Nb/Ce slab melt (Cooper et al., 2012). These correlations are difficult to explain if H_2O is controlled by degassing. Thus, while it is difficult to conceive how the crust would not affect the volatile history of ascending magma, correlations with slab proxies point to primary water information stored at some volcanoes, and a deeper control on water.

5. Mantle control on magmatic water

It is also possible that magmas emerge from the mantle with similar water contents. To evaluate this, melt inclusions are restored to primary compositions by adding olivine incrementally until melts are in equilibrium with mantle olivine of $\sim Fo_{90}$. Melt inclusions in hosts $<Fo_{80}$ are excluded from this treatment, because they likely have experienced fractionation of substantial amounts of other phases in addition to olivine. For those inclusions hosted in $>Fo_{80}$, the range of olivine addition is 0–20% (Table 1). The H_2O concentrations in the melt inclusions are then diluted by this amount of olivine addition, leading to a small correction (0–20%) to obtain $H_2O_{(Fo90)}$. The range in $H_2O_{(Fo90)}$ from arc to arc is 2.7 wt% (Kamchatka) to 4.2 wt% (Marianas), with the average of arcs being 3.4 ± 0.5 wt%. This average is shifted to lower concentrations than the original (3.9 ± 0.5 wt% H_2O) by about 15%, within the range of olivine added to calculate primary values. But importantly, the standard deviation remains the same, implying a similarly narrow range of H_2O values generated in the mantle. Why is the variation so small?

One possibility for the small variation in water content is the effect of water itself on the melting process. Water is a major element in arc magmas, and because of its low solubility in mantle minerals, it has a major effect on melting energetics. Tenths of a percent water in the mantle lowers the solidus by hundreds of degrees and can increase melt fraction by 10% (e.g., Katz et al., 2003). Moreover, there is a negative feedback in the wet melting process. At constant temperature and pressure, water contents in the source ($H_2O_{(o)}$) scale with melt fraction (F) such that the water contents of the melt ($H_2O_{(Fo90)}$) vary little. That is, higher $H_2O_{(o)}$ drives higher F, keeping $H_2O_{(Fo90)}$ similar to what would result from lower $H_2O_{(o)}$ at low F. Although the relationship between F and $H_2O_{(o)}$ is not strictly linear, but curved (Asimow and Langmuir, 2003; Langmuir et al., 2006), the generality above holds. The negative feedback of H_2O on its concentration in mantle melts provides one explanation for the narrow range in arc magmas.

The relationship between H_2O and F is illustrated in Fig. 6, with model curves for wet partial melting at constant P and T (following equations in Kelley et al. (2010), which are based on the approach in Langmuir et al. (2006)). Each curve shows increasing F with increasing $H_2O_{(o)}$. On a diagram such as this one, which plots $H_2O_{(o)}$ vs. F, the concentration of an incompatible element in the liquid (with partition coefficient, $D \sim 0$) is approximated by a line of constant slope that intersects the origin. H_2O satisfies this condition, with a D (mantle/liquid) that varies from 0.006 to 0.01 (Hirschmann et al., 2009). Thus, the batch melting equation, $C_L/C_o = 1/[F(1-D)+D]$, reduces to $C_L/C_o \sim 1/F$, and the slope $C_o/F \sim C_L$, or the liquid concentration. Dashed lines in Fig. 6 are lines of constant water content in the melt. This also illustrates how a compensatory relationship between $H_2O_{(o)}$ and F may lead to a narrow range of water contents of melts. In practice, this may occur during melting at nearly constant P and T, within a narrow range of melting curves. $H_2O_{(o)}$ may vary widely along one of these curves while the water content of the melt less so. For example, melts with 1.5–4.5 wt% H_2O (a factor of three) are generated from sources with 0.1–1.0 wt% H_2O (an order of

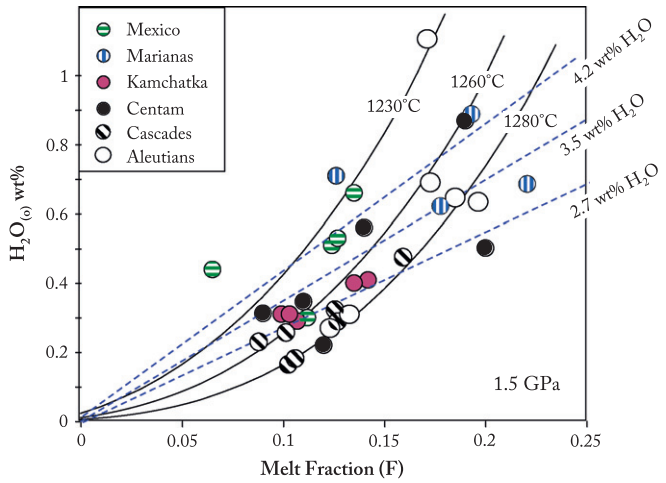

Fig. 6. Mantle melt fraction (F) vs. mantle water concentration, $H_2O_{(o)}$. Curved lines are calculated for wet melting at a single pressure (1.5 GPa) and temperature (as labeled) from equations in Kelley et al (2010). Dashed lines are constant water concentration in the melt (H_2O_L), which is approximately equal to the slope on this diagram (i.e., the batch melting equation, $H_2O_L/H_2O_o = 1/[F(1-D)+D]$ reduces to $H_2O_o/F \sim H_2O_L$ for $D \sim 0$). Data points for different arcs are as given in Johnson et al. (2009), Kelley et al. (2010), Portnyagin et al. (2007), Sadofsky et al. (2008) and Ruscitto et al. (2010). In other cases, F is calculated from TiO_2 concentration, after correcting to Fo_{90} compositions, and assuming 0.133 wt% TiO_2 in the mantle source and $D=0.04$, as in Kelley et al. (2006). $H_2O_{(o)}$ is calculated from F and $H_2O_{(L)}$. The anhydrous solidus at this pressure is 1308 °C (Hirschmann, 2000), and so all almost all the arc data plotted here require a major component of water-fluxed melting. The Tonga arc is not included here, as there is strong evidence for highly refractory (harzburgite) mantle beneath some regions of the arc (Cooper et al., 2010) , which leads to different wet melting curves than those shown here, and large variation in the inferred TiO_2 in the source, which makes F difficult to calculate. Consideration of the Tonga arc melting systematics will be explored in a future publication, after Cooper (2009).

magnitude) along the 1260 °C curve in Fig. 6. Thus, wet melting can generate melts with a limited range of water concentrations, even if the water concentration of the source and F vary substantially.

5.1. Testing the mantle control

This melting scenario can be tested by comparing $H_2O_{(o)}$ and F calculated for different arc volcanoes. One common procedure is to calculate F from the concentration of an incompatible, conservative element, like TiO_2 (which derives predominantly from the mantle and not the slab), and then calculate $H_2O_{(o)}$ from F and $H_2O_{(Fo90)}$ (Kelley et al., 2006; Portnyagin et al., 2007). Calculated in this way, arc data fall on a wide band across the melting diagram (Fig. 6), along lines with slopes that conform to the arc-averaged $H_2O_{(Fo90)}$ (3.4 ± 0.5 wt%). The data also lie within a narrow range of melting conditions, equivalent to mantle temperatures of 1230–1280 °C at 1.5 GPa. Other pressures and temperatures are possible, but all will show a narrow range of temperatures at constant pressure to produce the array. Although there is a pressure dependence to the melting systematics (Kelley et al., 2010; Hirschmann, 2010), the primary control is not absolute temperature, but the distance to the anhydrous solidus (Langmuir et al., 2006; Portnyagin et al., 2007). In units relative to the dry peridotite solidus (ΔT_{dps}), the model curves here represent melting at ΔT_{dpsH} of −30 to −80 °C (the H referring to the anhydrous solidus of Hirschmann (2000)).

These results are consistent with studies by Portnyagin et al. (2007), Johnson et al. (2009), and Ruscitto et al. (2010), for Kamchatka, Mexico and the Cascades, respectively, using this same treatment to estimate ΔT_{dpsH} values of −35 to −85 °C. Kelley et al. (2010) estimated lower ΔT_{dps} for the Marianas (−100 to −40 °C), but this is relative to a more refractory mantle solidus (Wasylenki et al., 2003) that is 39° above the Hirschmann (2000) solidus. The predominance of melting temperatures below the dry solidus is evidence for water-fluxed melting beneath most arc volcanoes. Such melting temperatures, however, fall within a narrow range (within 50 °C), and this prevalent temperature of the sub-arc mantle may be the ultimate cause of the limited water variation observed in arc magmas.

Fig. 6 also shows how different arcs may reflect distinctly different source concentrations in H_2O. For example, the Marianas and Mexican arcs both tap melts with 3.5–4.5 wt% $H_2O_{(Fo90)}$, and yet the Marianas source appears to be uniformly wetter (>0.6 wt% $H_2O_{(o)}$) than the Mexican sources (<0.6 wt% $H_2O_{(o)}$). More water in the Marianas source also apparently drives higher F (12–22%), and correlates with uniformly higher Ba/Nb (~200) than in Mexican magmas (<75). Thus $H_2O_{(o)}$ may reflect slab fluxes and melt volumes better than water contents in the magma.

Lastly, an additional test of the mantle melting model may come from independent estimates of the temperatures and pressures of primary arc magmas. Olivine–orthopyroxene–melt thermobarometers have been newly calibrated to incorporate the H_2O contents of mantle melts (e.g., Lee et al., 2009; Putirka, 2008), and recent applications using restored melt inclusion compositions suggest P and T conditions similar to those predicted from the H_2O–F systematics (Kelley et al., 2010; Ruscitto et al., 2010). Phase equilibrium laboratory experiments also provide an approach to constrain the conditions of melting. For example, Pichavant et al. (2002) concluded that primary melts from St. Vincent, Antilles corresponds to ΔT_{dpsH} of 0 to −100 °C (at 1.1–1.6 GPa). Other experiments on primitive arc magmas suggest ΔT_{dpsH} of −30 °C at ~1.5 GPa for the Aleutians and as much as −150 °C at 1.3 GPa (using the Wasylenki et al. (2003) solidus) for Mexico (Weaver et al., 2011). It is important to note, however, that both experimental results (Weaver et al., 2011) and melt inclusion thermobarometry (Ruscitto et al., 2012) suggest that melts produced in the hottest part of the wedge at least partially reequilibrate in the shallow mantle before ascending into the crust, so the ΔT_{dps} values above are minima. The results of these models and lab experiments suggest that even if a crustal water filter applies, mantle melting may deliver a fairly uniform product.

6. Implications and prospects for the future

There are many important problems, from global water fluxes to magma storage and eruption, that depend critically on whether the mantle or crust control magmatic water contents. If the common ~4 wt% H_2O average seen in mafic arc melt inclusions derives from a strong crustal filter, then it may be very difficult to ever estimate volatile fluxes from the mantle to the surface. Magmas could rise from the mantle with widely varying H_2O contents (anything >4 wt%) and then lose water on their way to storage at ~6 km. Any melt inclusions that were originally trapped at higher pressures might re-equilibrate by diffusive H loss through the olivine host at that depth, and if so, the only part of the volatile history of the magma that is recorded would involve the subsequent ascent, degassing and eruption above that depth, at water contents ≤4 wt%. The earlier history would be invisible, and the original water contents would be unmeasurable. Flux estimates based on 4 wt% H_2O in the melt would potentially grossly under-estimate the total flux of water from the mantle to the crust and atmosphere.

6.1. Are there wetter magmas that never erupt?

A strong crustal filter could completely bias the measurements we make. Basaltic andesite melts with very high H_2O contents

(> 10 wt%) would crystallize amphibole in the lower to middle crust (Grove et al., 2003) but may also die there from viscous death (Annen et al., 2006). The plutonic record could then be wetter than the eruptive record we have compiled here. There is some evidence for such a bias in the Mg#–SiO_2 relationships of arc plutonic vs. volcanic rocks (Kelemen, 1995), but as yet little quantitative data exist on the water contents of plutonic magmas. The presence of high Mg# amphibole in eruptive rocks may be a tell-tale sign of this missing output (Krawczynski et al., 2012), but such phenocrysts are rare in most arc magmas. On the other hand, Davidson et al. (2007) argue on the basis of arc REE patterns that amphibole is a nearly ubiquitous fractionating phase in lower crustal magmas but is nonetheless absent as a phenocryst in many volcanic suites. Thus, future work might focus on xenocrysts or antecrysts from the lower crust (e.g., Streck, et al., 2002), pyroxenes or amphiboles, that may retain in their structure earlier magmatic volatile contents. This approach holds promise, as pyroxenes may be more resistant to H_2O-re-equilibration than olivine-hosted melt inclusions (Wade et al., 2008; Peslier et al., 2002; Peslier and Luhr, 2006).

6.2. What is the crustal filter and does it limit explosive potential?

If the crustal water filter hypothesis is correct, then an important implication is that there must be a fundamental transition in the crust around 6 km, reflecting special conditions in crustal rheology, density and/or stress state. A related question is whether the maximum water contents of silicic magmas also reflect a crustal filter, resulting in similar depths of stalling for silicic magmas as for the predominantly mafic magmas studied here (Wallace, 2005). And if there is a crustal water filter, does this limit the gas content and explosive potential of magmas on our planet? Further integrated work linking different magma types and their volatile contents, with information on the geophysical structure of the crust and magma plumbing systems represents a rich new avenue of research that may illuminate the workings of a crustal water filter.

6.3. The link between H_2O content in melts and mantle P–T through the cryoscopic effect

If the mantle is the dominant control on magmatic water contents, then the limited range observed points to a regularity in the melting process. We have already demonstrated how water can modulate its concentration during H_2O-undersaturated melting of mantle peridotite, and how the narrow range observed in the water content of the melt might reflect a limited range in the *P–T* conditions within the melting region beneath different arcs. Wet melting (below the dry solidus) predominates and is restricted to a 50° range (30–80 °C below the dry solidus, Fig. 6) for the arcs investigated here. The underlying control is the temperature of the mantle wedge. Mantle that is 1250–1300 °C at 1.5 GPa (~50 km depth) will generate melts with ~3.5 wt% H_2O given current thermodynamic models—this is inherent to the cryoscopic effect. A given H_2O concentration in the melt will lead to a given freezing point depression of the appropriate melting contour (*F*). *F* in turn depends on $H_2O_{(o)}$, so there is no constant depression, but it is limited for plausible values of *F*. For example, 3.5 wt% H_2O in the melt depresses the melting temperature of peridotite (Hirschmann, 2010) or the olivine-saturated basalt liquidus (Medard and Grove, 2008) by ~110 °C. If *F* is in the range of 10–20%, this requires an increase in temperature of 40–80 °C above the dry solidus (Hirschmann, 2010), and so the two effects together lead a net depression of −30 to −70° below the dry solidus, or ΔT_{dps} of −30 to −70 °C, very similar to the calculations in Fig. 6. This outcome is a feature of all melting models that exploit the cryoscopic effect (e.g., Katz et al., 2003; Grove et al., 2006; Langmuir et al., 2006; Kelley et al., 2010; Hirschmann, 2010). A fully thermodynamic approach will lead to more accurate results over a wider range of compositions but is unlikely to change the primary conclusion that a limited range of H_2O concentrations in primary mantle melts requires a limited set of *P–T* conditions in the mantle wedge beneath arcs.

6.4. Comparison to numerical models of wedge thermal structure

Such a limited range in mantle wedge temperatures appears somewhat surprising, given the wide range in subduction parameters represented here (e.g., convergence rate, slab age). On the other hand, the numerical models of Syracuse et al. (2010) show that for a constant depth of slab–mantle coupling (80 km in their model), the maximum mantle wedge temperature beneath arcs falls within a limited range (1400 ± 54 °C 1 s.d.), the absolute value of which is mainly a function of the potential temperature assumed for mantle entering the wedge (1420 °C). Thus, it may be that the global combination of subduction parameters has a limited effect on maximum mantle wedge temperatures. Moreover, the ΔT_{dpsH} calculated from the Syracuse et al. (2010) model (-66 ± 42 °C) encompasses the same range as we calculated above, based on observed H_2O contents. In a similar numerical study, England and Katz (2010) argue that the largest melt fractions may occur in the mantle wedge along a *P–T* array that parallels the dry solidus. As our cryoscopic argument highlights, such an array will lead to melts with a narrow range of water contents, like those observed. Thus, there is some support for the England and Katz (2010) model in the water contents of arc magmas, although their predicted temperatures ($\Delta T_{dpsH} = -100$ to -150) are much lower than those predicted here or from olivine–opx–melt thermobarometry (Kelley et al., 2010; Ruscitto et al., 2010). None of these numerical models, however, predict mantle wedge temperatures as low as the "cold plume" models (e.g., Vogt et al., 2012) that generate melt at temperatures far below the ΔT_{dps} values predicted here. These comparisons highlight the importance of knowing primary water contents in constraining the *P–T* path of mantle melting above subduction zones.

If the relative constancy in the water content of average arc magmas reflects a relative constancy in the *P–T* conditions within the mantle wedge, then the ultimate modulator may then be the average temperature of the upper mantle. Like the nearly uniform thickness of the oceanic crust, perhaps the small range in the water contents of arc magmas is another reflection of a planet with a background uniform potential temperature ~1400 °C.

6.5. Implications for global H_2O recycling fluxes

If arc magmas rise from the mantle with ~3–4% H_2O on average, this makes trivial many important flux calculations. For example, the water output flux at arcs would then simply be 3.4% (global $H_2O_{(Fo90)}$) of the magma production rate (on a mass basis), which is not well known, but most estimates (on a volume basis) lie around 2–4 km^3/yr (Reymer and Schubert, 1984; Crisp, 1984; Dimalanta et al., 2002). This yields $1.9–3.8 \times 10^8$ Tg/Myr H_2O output at arcs, which agrees generally with estimates based on gas fluxes (3×10^8 Tg/Myr, Wallace, 2005), and with the predicted total water losses from subducting slabs by the time they reach ~100 km depth, based on coupled thermal and thermodynamic models for slab *P–T*–H_2O paths (3.2×10^8 Tg/Myr; van Keken et al., 2011). Thus, recycling to the arc over the first 100 km of subduction may be nearly 100% efficient, stemming the loss of the oceans down the subduction zone through time (Rupke et al., 2004; Parai and Mukhopodhyay, 2012). The water content of the mantle residual to arc melting would then be ~34,000 ppm

$H_2O \times D_{H2O}$(peridotite/liq) (0.006–0.008; Hirschmann et al., 2009), or 200–300 ppm H_2O. Such mantle, even after melt removal, would be wetter, weaker and more attenuating to seismic waves that the average upper mantle that upwells beneath mid-ocean ridges (Hirth and Kohlstedt, 2004).

6.6. The diversity of water contents in magmas parental to arc volcanoes

Although we have emphasized in this paper the surprisingly narrow range in the average H_2O contents of volcanic arcs, the variations observed from volcano to volcano are still highly significant, and clearly give rise to a diversity of magma chemistry and eruptive styles greater than that found in other tectonic settings. For example, the difference between 2 and 6 wt% H_2O is very large in terms of phase equilibria (Grove et al., 2012), affecting amphibole, plagioclase and spinel-phase crystallization in particular, and responsible for the entire range of crystal fractionation trends from tholeiitic to calc-alkaline (Zimmer et al. 2010). The factor of three range may also be a primary control on the explosive potential of an eruption (Roggensack et al., 1997). Thus, there is still immense value in measuring water contents for different magma series and in different eruptive products.

It is also likely that greater diversity exists in the volatile content of magmas parental to a given volcano than we have compiled here. We selected from each melt inclusion population only the highest H_2O content for each volcano, assuming the lower H_2O contents have a secondary cause (usually degassing) and not a primary one (from the mantle). It is possible, however, that some melt inclusions with lower H_2O contents reflect drier initial magmas, and so our averaging could be biased to the wettest magmas that feed each volcano. Such questions of initial magma diversity can be evaluated to some degree by careful examination of incompatible element ratios in melt inclusions, which will not be fractionated by degassing but will potentially vary in different primary melts. Such analysis in many cases reveals a common parentage to all melt inclusions and bulk rocks from a single eruption. For example, Ba/Zr in Fuego melt inclusions are identical to one another, and to the bulk tephra (Lloyd et al., 2013), thus supporting a common parental magma to all. In this case, it is likely that the parental magma also had a single H_2O concentration, and that the H_2O variations observed are secondary in origin. The same is true for melt inclusion suites from many other arc volcanoes (e.g., Arenal volcano; Wade et al., 2006; Irazu volcano, Benjamin et al., 2007), which is in stark contrast to the diversity more commonly reported in melt inclusions suites from ocean islands (e.g., Sobolev et al., 2000; Maclennan et al., 2003) and MORB (e.g., Sobolev and Shimizu, 1993; Laubier et al., 2012). Whether this is due to the more efficient blending of melts in arc plumbing systems, or a lack of data on near-primary melts or samples from isolated vents, is an area for future effort.

Resolving the relative importance of crust and mantle control on magmatic water contents will require new efforts in coupling volatiles to trace element and isotopic variations, examining H_2O–CO_2 degassing relationships, measuring H_2O and trace elements in primitive phenocrysts, and combining petrological and geophysical studies of magma plumbing systems that extend to mantle depths.

Acknowledgments

This paper was motivated by talks given at the 2009 MARGINS Volatiles Institute and the 2010 CIDER workshop, both supported by the US National Science Foundation, which also has supported our work over the last decade on arc volatile contents (NSF-OCE-0001897, OCE-0526450, OCE-0549051, EAR-0609953, EAR-0309559 and EAR-0440394). We thank Mark Reagan, Becky Lange, Maxim Portnyagin, Elizabeth Cottrell, Glenn Gaetani, Charlie Langmuir, Ed Stolper, Tim Grove, Jon Blundy, Dan Ruscitto and Alison Shaw for stimulating discussions on this topic over the years; Leonid Danyushevsky for all manner of help; and Marc Hirschmann and an anonymous reviewer for their insightful reviews.

Appendix A. Supporting information

Supplementary data associated with this article can be found in the online version at http://dx.doi.org/10.1016/j.epsl.2012.11.044.

References

Anderson, A.T., 1973. The before-eruption water contents of some high-alumina magmas. Bull. Volcanol. 37, 530–552.
Anderson, A.T., 1974a. Evidence for a picritic, volatile-rich magma beneath Mt. Shasta, California. J. Petrol. 15, 243–267.
Anderson, A.T., 1974b. Chlorine, sulfur and water in magmas and oceans. Geol. Soc. Am. Bull. 85, 1492–1585.
Anderson, A.T., 1976. Magma mixing: petrological process and volcanological tool. J. Volcanol. Geotherm. Res. 1, 3–33.
Annen, C., Blundy, J.D., Sparks, R.S.J., 2006. The genesis of intermediate and silicic magmas in deep crustal hot zones. J. Petrol. 47, 505–539.
Asimow, P.D., Langmuir, C.H., 2003. The importance of water to oceanic mantle melting regimes. Nature 421, 815–820.
Auer, S., Bindeman, I., Wallace, P.J., Ponomareva, V., Portnyagin, M., 2009. The origin of hydrous, high-$d^{18}O$ voluminous volcanism: diverse oxygen isotope values and high magmatic water contents within the volcanic record of Klyuchevskoy volcano, Kamchatka, Russia. Contrib. Mineral. Petrol. 157, 209–230, http://dx.doi.org/10.1007/s00410-008-0330-0.
Benjamin, E.R., Plank, T., Wade, J.A., Kelley, K.A., Hauri, E.H., Alvarado, G.E., 2007. High water contents in basaltic magmas from Irazu Volcano, Costa Rica. J. Volcanol. Geotherm. Res. 168, 68–92.
Blundy, J., Cashman, K.V., 2005. Rapid decompression crystallization recorded by melt inclusions from Mount St. Helens volcano. Geology 33, 793–796.
Blundy, J., Cashman, K., Humphreys, M., 2006. Magma heating by decompression-driven crystallization beneath andesite volcanoes. Nature 443, 76–80.
Carmichael, I.S.E., 2002. The andesite aqueduct: perspectives on the evolution of intermediate magmatism in west-central (105–99°W) Mexico. Contrib. Mineral. Petrol. 143, 641–663.
Cashman, K.V., 2004. Volatile controls on magma ascent and degassing. The state of the planet: frontiers and challenges in geophysics. Am. Geophys. Union Mon. 150, 109–124.
Caulfield, J.T., Turner, S.P., Smith, I.E.M., Cooper, L.B., Jenner, G.A., 2012. Magma evolution in the primitive. intra-oceanic Tonga Arc: petrogenesis of basaltic andesites at Tofua Volcano. J. Petrol 53, 1197–1230, http://dx.doi.org/10.1093/petrology/egs013.
Cervantes, P., Wallace, P.J., 2003. Role of H_2O in subduction-zone magmatism: new insights from melt inclusions in high-Mg basalts from central Mexico. Geology 31, 235–238.
Cervelli, P.F., Fournier, T.J., Freymueller, J.T., Power, J.A., Lisowski, M., Pauk, B.A., 2010. Geodetic constraints on magma movement and withdrawal during the 2006 eruption of Augustine Volcano. Chapter 17 in The 2006 Eruption of Augustine Volcano, Alaska; Power, J.A., Coombs, M.L., Freymueller, J.T. (Eds.), USGS Professional Paper 1769.
Chen, Y., Provost, A., Schiano, P., Cluzel, N., 2011. The rate of water loss from olivine-hosted melt inclusions. Contrib. Mineral. Petrol. 162, 625–636, http://dx.doi.org/10.1007/s00410-011-0616-5.
Clocchiatti, R., 1968. Morphology of vitrous inclusions in quartz phenocrystals of acid lava of northern Vosges mountains. Comptes Rendus Hebdomadaires des Seances de l Academie des Sciences Serie D 267 (26), 2257.
Clocchiatti, R., Desnoyers, C., Pyel, P., 1975. Relation between magmatic inclusions and properties of anorthoses from Erebus. Bull. Soc. Franc. Mineral. Cristall. 98, R25–R26.
Contreras-Reyes, E., Grevemeyer, I., Watts, A.B., Flueh, E.R., Peirce, C., Moeller, S., Papenberg, C., 2011. Deep seismic structure of the Tonga subduction zone: implications for mantle hydration, tectonic erosion, and arc magmatism. J. Geophys. Res. 116, B10103, http://dx.doi.org/10.1029/2011JB008434.
Cooper, L.B., 2009. Volatiles in Tonga Arc Magmas and their Role in Unraveling Subduction Zone Processes. Ph.D. Dissertation. Boston University.
Cooper, L.B., Plank, T., Arculus, R.J., Hauri, E.H., Hall, P.S., Parman, S.W., 2010. High-Ca boninites from the active Tonga Arc. J. Geophys. Res. 115, B10206, http://dx.doi.org/10.1029/2009JB006367.

Cooper, L.B., Ruscitto, D., Plank, T., Wallace, P.J., Syracuse, E., Manning, C.E., 2012. Global variations in H_2O/Ce I: slab surface temperatures beneath volcanic arcs. Geochem. Geophys. Geosyst. 13, Q03024, http://dx.doi.org/10.1029/2011GC003902 27 pp.

Crisp, J.A., 1984. Rates of magma emplacement and volcanic eruption. J. Volcanol. Geotherm. Res. 20, 177–211.

Danyushevsky, L.V., Falloon, T.J., Sobolev, A.V., Crawford, A.J., Carroll, M., Price, R.C., 1993. The H_2O content of basalt glasses from southwest Pacific back-arc basins. Earth Planet. Sci. Lett. 117, 347–362.

Davidson, J., Turner, S., Handley, H., MacPherson, C., Dosseto, A., 2007. Amphibole 'sponge' in arc crust? Geology 35, 787–790.

Dimalanta, C., Taira, A., Yumul, G.P., Tokuyama, H., Mochizuki, K., 2002. New rates of western Pacific island arc magmatism from seismic and gravity data. Earth Planet. Sci. Lett. 202, 105–115.

England, P.C., Katz, R.F., 2010. Melting above the anhydrous solidus controls the location of volcanic arcs. Nature 467, 700–703, http://dx.doi.org/10.1038/nature09417.

Gaetani, G.A., O'Leary, J.A., Shimizu, N., Bucholz, C.E., Newville, M, 2012. Rapid re-equilibration of H_2O and oxygen fugacity in olivine-hosted melt inclusions. Geology, 40, 915–918, http://dx.doi.org/10.1130/G32992.1.

Gonnermann, H.M., Manga, M., 2007. The fluid mechanics inside a volcano. Ann. Rev. Fluid Mech. 39, 321–356.

Grove, T.L., Elkins-Tanton, L.T., Parman, S.W., Chatterjee, N., Muntener, O., Gaetani, G.A., 2003. Fractional crystallization and mantle-melting controls on calc-alkaline differentiation trends. Contrib. Mineral. Petrol. 145, 515–533.

Grove, T.L., Baker, M.B., Price, R.C., Parman, S.W., Elkins-Tanton, L.T, Chatterjee, N., Muntener, O., 2005. Magnesian andesite and dacite lavas from Mt. Shasta, northern California: products of fractional crystallization of H_2O-rich mantle melts. Contrib. Mineral. Petrol. 148, 542–565.

Grove, T.L., Chatterjee, N., Parman, S.W., Medard, E., 2006. The influence of H_2O on mantle wedge melting. Earth Planet. Sci. Lett. 249, 74–89, http://dx.doi.org/10.1016/j.epsl.2006.06.043.

Grove, T.L., Till, C.B., Krawczynski, M.J., 2012. The role of H_2O in subduction zone magmatism. Annu. Rev. Earth. Planet. Sci. 40, 413–439.

Hauri, E.H., Shaw, A., Gaetani, G., Plank, T., Kelley, K., Wade, J., O'Leary, J., 2007. Subduction Factory: Understanding the Role of Water Flux in Arc Systems. MARGINS Newsletter #18, pp. 1–5.

Hauri, E.H., Weinreich, T., Saal, A.E., Rutherford, M.C., Van Orman, J.A., 2011. High pre-eruptive water contents preserved in lunar melt inclusions. Science 333, 213–215.

Hirth, G., Kohlstedt, D.L., 1996. Water in the oceanic upper mantle: implications for rheology, melt extraction and the evolution of the lithosphere. Earth Planet. Sci. Lett. 144, 93–108, http://dx.doi.org/10.1016/0012-821X(96)00154-9.

Hirth, G., Kohlstedt, D.L., 2004. Rheology of the upper mantle and the mantle wedge: a view from the experimentalists, in Inside the Subduction Factory. In: Eiler, J. (Ed.), Geophysical Monograph Series, 138. American Geophysical Union, Washington, DC, pp. 83–106.

Hirschmann, M.M., 2000. Mantle solidus: experimental constraints and the effects of peridotite composition. Geochem. Geophys. Geosyst. 1, http://dx.doi.org/10.1029/2000GC000070.

Hirschmann, M.M., Tenner, T., Aubaud, C., Withers, A.C., 2009. Dehydration melting of nominally anhydrous mantle: the primacy of partitioning. Phys. Earth Planet. Inter. 176, 54–68, http://dx.doi.org/10.1016/j.pepi.2009.04.001.

Hirschmann, M.M., 2010. Partial melt in the oceanic low velocity zone. Phys.. Earth Planet. Inter. 179, 60–71.

Johnson, E.R., Wallace, P.J., Cashman, K.V., Delgado-Granados, H., Kent, A.J.R., 2008. Magmatic volatile contents and degassing-induced crystallization at Volcán Jorullo, Mexico: implications for melt evolution and the plumbing systems of monogenetic volcanoes. Earth Planet. Sci. Lett. 269, 477–486.

Johnson, E.R., Wallace, P.J., Delgado-Granados, H., Manea, V.C., Kent, A.J.R., Bindeman, I.N., Donegan, C.S., 2009. Subduction-related volatile recycling and magma generation beneath Central Mexico: insights from melt inclusions, oxygen isotopes and geodynamic models. J. Petrol. 50, 1729–1764.

Johnson, E.R., Wallace, P.J., Cashman, K.V., Delgado Granados, H., 2010. Degassing of volatiles (H_2O, CO_2, S, Cl) during ascent, crystallization, and eruption at mafic monogenetic volcanoes in central Mexico. J. Volcanol. Geotherm. Res. 197, 225–238.

Katz, R.F., Spiegelman, M., Langmuir, C.H., 2003. A new parameterization of hydrous mantle melting. Geochem. Geophys. Geosyst. 4, 1073.

Kelemen, P.B., 1995. Genesis of high Mg# andesites and the continental crust. Contrib. Mineral. Petrol. 120, 1–19.

Kelley, K.A., Plank, T., Newman, S., Stolper, E., Grove, T.L., Hauri, E., 2006. Mantle melting as a function of water content at subduction zones. I: back-arc basins. J. Geophys. Res. 111, B09208.

Kelley, K.A., Plank, T., Newman, S., Stolper, E., Grove, T.L., Parman, S., Hauri, E., 2010. Mantle melting as a function of water content beneath the Mariana arc. J. Petrol. 51, 1711–1738, http://dx.doi.org/10.1093/petrology/egq036.

Krawczynski, M.J., Grove, T.L., Behrens, H., 2012. Amphibole stability in primitive arc magmas: effects of temperature, H_2O content, and oxygen fugacity. Contrib. Mineral. Petrol. 164, 317–339.

Langmuir, C.H., Bezos, A., Escrig, S., Parman, S.W., 2006. Chemical systematics and hydrous melting of the mantle in back-arc basins. In: Christie, D.M., Fisher, C.R., Lee, S.-M., Givens, S. (Eds.), Back-arc Spreading Systems: Geological, Biological, Chemical, and Physical Interactions. American Geophysical Union Geophysical Monograph Series 166, pp. 87–146.

Laubier, M., Gale, A., Langmuir, C.H., 2012. Melting and crustal processes at the FAMOUS segment (mid-atlantic ridge): new insights from olivine-hosted melt inclusions from multiple samples. J. Petrol. 53, 665–698.

Lee, C.-T.A., Luffi, P., Plank, T., Dalton, H., Leeman, W.P., 2009. Constraints on the depths and temperatures of basaltic magma generation on Earth and other terrestrial planets using new thermobarometers. Earth Planet. Sci. Lett. 279, 20–33, http://dx.doi.org/10.1016/j.epsl.2008.12.020.

Lloyd, A.S., Plank, T., Ruprecht, P., Hauri, E., Rose, W., 2013. Volatile loss from melt inclusions in pyroclasts of differing sizes. Contrib. Mineral. Petrol. 165, 129–153, http://dx.doi.org/10.1007/s00410-012-0800-2.

Lu, Z., Dzurisin, D., Biggs, J., Wicks, C., McNutt, S., 2010. Ground surface deformation patterns, magma supply, and magma storage at Okmok volcano, Alaska, from InSAR analysis: 1. Intereruption deformation, 1997–2008. J. Geophys. Res. 115, B00B02, http://dx.doi.org/10.1029/2009JB006969.

Maclennan, J., McKenzie, D., Hilton, F., Gronvold, K., Shimizu, N., 2003. Geochemical variability in a single flow from northern Iceland. J. Geophys. 108 (B1), 2007, http://dx.doi.org/10.1029/2000JB000142.

Massare, D., Metrich, N., Clocchiatti, R., 2002. High-temperature experiments on silicate melt inclusions in olivine at 1 atm: inference on temperatures of homogenization and H_2O concentrations. Chem. Geol. 183, 87–98.

Medard, E., Grove, T.L., 2008. The effect of H_2O on the olivine liquidus of basaltic melts: experiments and thermodynamic models. Contrib. Mineral. Petrol. 155, 417–432.

Mercier, M., Di Muroc, A., Metrich, N., Giordano, D., Belhadja, O., Mandeville, C.W., 2010. Spectroscopic analysis (FTIR, Raman) of water in mafic and intermediate glasses and glass inclusions. Geochim. Cosmochim. Acta 74, 5641–5656.

Metrich, N., Bertagnini, A., Di Muro, A., 2010. Conditions of magma storage, degassing and ascent at Stromboli: new insights into the volcano plumbing system with inference on the eruptive dynamics. J. Petrol. 51, 603–626.

Mosenfelder, J.L., Le Voyer, M., Rossman, G.R., Guan, Y., Bell, D.R., Asimow, P.D., Eiler, J.M., 2011. Analysis of hydrogen in olivine by SIMS: evaluation of standards and protocol. Am. Mineral. 96, 1725–1741.

Newman, S., Lowenstern, J.B., 2002. VOLATILECALC: a silicate–melt–H_2O–CO_2 solution model written in Visual Basic for Excel. Comput. Geosci. 28, 597–604.

Parai, R., Mukhopadhyay, S., 2012. How large is the subducted water flux? New constraints on mantle regassing rates. Earth Planet. Sci. Lett. 317–8, 396–406.

Peslier, A.H., Luhr, J.F., Post, J., 2002. Low water contents in pyroxenes from spinelperidotites of the oxidized, subarc mantle wedge. Earth Planet. Sci. Lett. 201, 6986.

Peslier, A.H., Luhr, J.F., 2006. Hydrogen loss from olivines in mantle xenoliths from Simcoe (USA) and Mexico: mafic alkalic magma ascent rates and water budget of the subcontinental lithosphere. Earth Planet. Sci. Lett. 242, 302–319.

Pichavant, M., Mysen, B.O., MacDonald, R., 2002. Source and H_2O content of high-MgO magmas in island arc settings: an experimental study of a primitive calc-alkaline basalt from St. Vincent, Lesser Antilles arc. Geochim. Cosmochim. Acta 66, 2193–2209, http://dx.doi.org/10.1016/S0016-7037(01)00891-2.

Plank, T., Langmuir, C.H., 1993. Tracing trace elements from sediment input to volcanic output at subduction zones. Nature 362, 739–743.

Plank, T., 2005. Constraints from Th/La on sediment recycling at subduction zones and the evolution of the continents. J. Petrol. 46, 921–944, http://dx.doi.org/10.1093/petrology/egi005.

Plank, T., Cooper, L., Manning, C.E., 2009. New geothermometers for estimating slab surface temperatures. Nat. Geosci. 2, 611–615.

Portnyagin, M., Hoernle, K., Plechov, P., Mironov, N., Khubunaya, S., 2007. Constraints on mantle melting and composition and nature of slab components in volcanic arcs from volatiles (H_2O, S, Cl, F) and trace elements in melt inclusions from the Kamchatka Arc. Earth Planet. Sci. Lett. 255, 53–69.

Portnyagin, M., Almeev, R., Matveev, S., Holtz, F., 2008. Experimental evidence for rapid water exchange between melt inclusions in olivine and host magma. Earth Planet. Sci. Lett. 272, 541–552.

Putirka, K.D., 2008. Thermometers and barometers for volcanic systems. In: Putirka, K.D., Tepley, F. (Eds.), Minerals, Inclusions and Volcanic Processes: Min. Soc. Am., Rev. Min. Geochem. 69, 61–120, doi: 10.2138/rmg.2008.69.3.

Reymer, A., Schubert, G., 1984. Phanerozoic addition rates to the continental crust and crustal growth. Tectonics 3, 63–77.

Roberge, J., Delgado Granados, H., Wallace, P.J., 2009. Mafic magma recharge supplies high CO_2 and SO_2 gas fluxes from Popocatepetl volcano, Mexico. Geology 37, 107–110.

Roggensack, K., Hervig, R.L., McKnight, S.B., Williams, S.N., 1997. Explosive basaltic volcanism from Cerro Negro volcano: influence of volatiles on eruptive style. Science 277, 1639–1642.

Rupke, L.H., Morgan, J.P., Hort, M., Connolly, J.A.D., 2004. Serpentine and the subduction zone water cycle. Earth Planet. Sci. Lett. 223, 17–34.

Ruscitto, D.M., Wallace, P.J., Johnson, E.R., Kent, A.J.R., Bindeman, I.N., 2010. Volatile contents of mafic magmas from cinder cones in the Central Oregon High Cascades: implications for magma formation and mantle conditions in a hot arc. Earth Planet. Sci. Lett. 298, 153–161.

Ruscitto, D.M., Wallace, P.J., Kent, A.J.R., 2011. Revisiting the compositions and volatile contents of olivine-hosted melt inclusions from the Mount Shasta region: implications for the formation of high-Mg andesites. Contrib. Mineral. Petrol. 162, 109–132, http://dx.doi.org/10.1007/s00410-010-0587-y.

Ruscitto, D., Wallace, P.J., Cooper, L., Plank, T., 2012. Global Variations in H_2O/Ce II: relationships to arc magma geochemistry and volatile fluxes. Geochem. Geophys. Geosyst. 13, Q03025, http://dx.doi.org/10.1029/2011GC003887.

Sadofsky, S.J., Portnyagin, M., Hoernle, K., van den Bogaard, P., 2008. Subduction cycling of volatiles and trace elements through the Central American volcanic arc: evidence from melt inclusions. Contrib. Mineral. Petrol. 155, 433–456.
Scandone, R., Cashman, K.V., Malone, S.D., 2007. Magma supply, magma ascent and the style of volcanic eruptions. Earth Planet. Sci. Lett. 253, 513–529.
Shaw, A.M., Hauri, E.H., Fischer, T.P., Hilton, D.R., Kelley, K.A., 2008. Hydrogen isotopes in Mariana arc melt inclusions: implications for subduction dehydration and the deep-Earth water cycle. Earth Planet. Sci. Lett. 275, 138–145.
Sisson, T.W., Layne, G.D., 1993. H_2O in basalt and basaltic andesite glass inclusions from four subduction-related volcanoes. Earth Planet. Sci. Lett. 117, 619–635.
Sobolev, A.V., Tsamerian, O.P., Zakariadze, G.S., Shcherbovskii, A.J., 1983. Compositions and conditions of the crystallization of the Lesser Caucasus Ophiolite volcanogenic complex melts according to the data of melt inclusion study. Dok. Akad. Nauk SSSR 272, 464–468.
Sobolev, A.V., Shimizu, N., 1993. Ultra-depleted primary melt included in an olivine from the Mid-Atlantic Ridge. Nature 363, 151–154.
Sobolev, A.V., Chaussidon, M., 1996. H_2O concentrations in primary melts from suprasubduction zones and mid-ocean ridges; implications for H_2O storage and recycling in the mantle. Earth Planet. Sci. Lett. 137, 45–55, http://dx.doi.org/10.1016/0012-821X(95)00203-O.
Sobolev, A.V., Hofmann, A.W., Nikogosian, I.K., 2000. Recycled oceanic crust observed in 'ghost plagioclase' within the source of Mauna Loa lavas. Nature 404, 986–989.
Spilliaert, N., Allard, P., Metrich, N., Sobolev, A.V., 2006. Melt inclusion record of the conditions of ascent, degassing and extrusion of basalt during the powerful 2002 flank eruption of Mount Etna (Italy). J. Geophys. Res. 111, B04203.
Stolper, E., Newman, S., 1994. The role of water in the petrogenesis of Mariana trough magmas. Earth Planet. Sci. Lett. 121, 293–325.
Streck, M.J., Dungan, M.A., Malavassi, E., Reagan, M.K., Bussy, F., 2002. The role of basalt replenishment in the generation of basaltic andesites of the ongoing activity at Arenal volcano, Costa Rica: evidence from clinopyroxene and spinel. Bull. Volcanol. 64, 316–327.
Syracuse, E.M., Van Keken, P.E., Abers, G.A., 2010. The global range of subduction zone thermal models. Phys. Earth Planet. Inter. 183, 73–90, http://dx.doi.org/10.1016/j.pepi. 2010.02.004.
van Keken, P.E., Hacker, B.R., Syracuse, E.M., Abers, G.A., 2011. Subduction factory: 4. Depth-dependent flux of H_2O from subducting slabs worldwide. J. Geophys. Res. 116, B01401, http://dx.doi.org/10.1029/2010JB007922.
Vigouroux, N., Wallace, P.J., Kent, A.J.R., 2008. Volatiles in high-K magmas from the western Trans-Mexican Volcanic Belt: evidence for fluid fluxing and extreme enrichment of the mantle wedge by subduction processes. J. Petrol. 49, 1589–1618.
Vogt, K., Gerya, T.V., Castro, A., 2012. Crustal growth at active continental margins: numerical modeling. Phys. Earth Planet. Inter. 192, 1–20.
Wade, J.A., Plank, T., Melson, W.G., Soto, G.J., Hauri, E., 2006. The volatile content of magmas from Arenal volcano. J. Volcanol. Geotherm. Res. 157, 94–120.
Wade, J., Plank, T., Zimmer, M., Hauri, E., Roggensack, K., Kelley, K., 2008. Prediction of magmatic water contents via measurement of H_2O in clinopyroxene phenocrysts. Geology 36, 799–802.
Walker, J.A., Roggensack, K., Patino, L.C., Cameron, B.I., Matais, O., 2003. The water and trace element contents of melt inclusions across an active subduction zone. Contrib. Mineral. Petrol. 146, 62–77.
Wallace, P.J., 2005. Volatiles in subduction zone magmas: concentrations and fluxes based on melt inclusion and volcanic gas data. J. Volcanol. Geotherm. Res. 140, 217–240.
Wasylenki, L.E., Baker, M.B., Kent, A.J.R., Stolper, E.M., 2003. Near-solidus melting of the shallow upper mantle: partial melting experiments on depleted peridotite. J. Petrol. 44, 1163–1191.
Weaver, S.L., Wallace, P.J., Johnston, A.D., 2011. A comparative study of continental vs. intraoceanic arc mantle melting: experimentally determined phase relations of hydrous primitive melts. Earth Planet. Sci. Lett. 308, 97–106.
Witham, F., Blundy, J., Kohn, S., Lesne, P., Dixon, J., Churakov, S.V., Botcharnikov, R., 2012. SolEx: a model for mixed COHSCl-volatile solubilities and exsolved gas compositions in basalt. Comput. Geosci. 45, 87–97, http://dx.doi.org/10.1016/j.cageo.2011.09.021.
Zimmer, M.M., Plank, T., Freymueller, J., Hauri, E.H., Larsen, J.F., Nye, C.J., 2007. Why do Magmas Stall? Insights from Petrologic and Geodetic Data. Eos Trans. AGU, 88(52), Fall Meet. Suppl., Abstract V41F-02.
Zimmer, M. M., 2008. Water in Aleutian Magmas: Its Origin in the Subduction Zone and its Effects on Magma Evolution. Ph.D. Thesis. Boston University, Boston, MA, 448 pp.
Zimmer, M.M., Plank, T., Hauri, E.H., Yogodzinski, G.M., Stelling, P., Larsen, J., Singer, B., Jicha, B., Mandeville, C., Nye, C.J., 2010. The role of water in generating the calc-alkaline trend: new volatile data for Aleutian magmas and a new tholeiitic index. J. Petrol. 51, 2411–2444, http://dx.doi.org/10.1093/petrology/egq062.

Terry Plank is a Professor of Geochemistry in the Department of Earth and Environmental Sciences of Columbia University and at the Lamont-Doherty Earth Observatory. She received an AB degree in Earth Sciences from Dartmouth College and a Ph.D. in Geoscience from Columbia University. Her current research focuses on the volatile contents of magmas, recycling of material at subduction zones, timescales of magma ascent and eruption, and integrating petrological and seismological observations of melting regions in the mantle.

Katherine A. Kelley is an Associate Professor of Oceanography at the Graduate School of Oceanography of the University of Rhode Island. She received a BA degree in Geology from Macalester College and a Ph.D. in Earth Sciences from Boston University. Her current research focuses on the budgets and cycling of magmatic volatiles, mantle and magmatic processes at convergent and divergent margins, and the balance of oxygen between the Earth's surface and interior.

Mindy M. Zimmer is a postdoc at Los Alamos National Laboratory. She received a BA in Geological Sciences from Michigan State University, an MS in Earth and Planetary Sciences from the University of New Mexico, and a Ph.D. from Boston University. Currently she works in the Nuclear and Radiochemistry group, applying her analytical geochemistry skills to the field of nuclear forensics.

Erik H. Hauri is a Staff Scientist in Geochemistry in the Department of Terrestrial Magnetism at the Carnegie Institution of Washington. He received a BS degree in Marine Geosciences at the University of Miami and a Ph.D. in Geoscience from the Massachusetts Institute of Technology and the Woods Hole Oceanographic Institution. He is currently the Chair of the Reservoirs & Fluxes Directorate of the Deep Carbon Observatory, an international decadal program focused on the Earth's deep carbon cycle. His current research focuses on the volatile cycles of the Earth, Moon and Mars, the nature of magma migration and eruption, the thermal and chemical evolution of the Earth's interior, and the fundamental chemical behavior of water, carbon and other volatiles under the pressure–temperature conditions of planetary interiors.

Paul J. Wallace is a Professor of Volcanology and Petrology in the Department of Geological Sciences at the University of Oregon. He received a BS in Geology from George Washington University and a Ph.D. in Geology from the University of California at Berkeley. His current research focuses on volatiles in subduction zone magmas and the relationship between shallow degassing processes, crystallization, and eruption styles.